

New Cascaded Architecture for Classical and Quantum Multiparameter Sensing

Gregory Krueper,¹ Lior Cohen,² and Juliet T. Gopinath^{1,2}

¹*Department of Physics, University of Colorado Boulder, Boulder CO 80309, USA*

²*Department of Electrical, Computer and Energy Engineering,
University of Colorado Boulder, Boulder CO 80309, USA*

We present an innovative concept for quantum-enhanced multiparameter optical phase sensing that can be implemented in free space, optical fiber or on-chip. Our measurable phases are in series, or cascaded, enabling measurements as a function of position with only a single input and output. We have modeled up to 20 phases, and fitting shows near-linear scaling of the power requirements for additional phases. This novel approach represents a new paradigm in multiparameter quantum metrology, and can be applied to remote sensing, communications, and geophysics.

In optical interferometers, the sensitivity of an optical phase measurement scales ideally as $n^{-1/2}$, where n is the number of photons. However, these measurements can be enhanced with quantum metrology, where this limit can be surpassed. For example, squeezed states of light can enhance the sensitivity by a factor of e^{2r} where r is the squeezing strength [1–3]. One of the most famous applications for these ultrasensitive interferometers is LIGO [4], but other applications include biological particle tracking [5], magnetometry [6], and optical gyroscopes [7].

More recently, multiparameter quantum estimation was developed [8–13]. Applications range from phase imaging and cold atom measurements to quantum networks [14–17]. In the above references, the estimation was done in parallel, where a probe is split into many branches to enable many concurrent measurements. However, a series (or cascaded) sensing scheme was not considered. The cascaded scheme enables compact multiparameter sensing in difficult to reach locations and allows conservation of resources. An example in classical sensors is with optical time domain reflectometry (OTDR) for optical fibers [18]. To our knowledge, no quantum analogue to OTDR is available today.

In this letter, we develop the framework for quantum cascaded phase sensing. Unlike many other quantum sensing schemes that use very low photon number, we design the sensor to use laser light and suppress its noise by squeezing. We calculate the classical multiparameter Fisher information for sensing all parameters for a lower bound on the measurement sensitivity. We show that additional phases require a near-linear intensity increase to achieve the same sensitivity. As an example, we demonstrate the physics of the sensor with numerical results of two and three-phase sensors, showing that information can be extracted with a quantum enhancement from partially distinguishable parameters. This novel concept is of interest not only for distributed fiber sensing, but also for integrated and free-space measurements. More generally, any quantum metrology scheme that senses many similar parameters could benefit from these techniques. It may also generalize to parameter estimation in a more

complex network [19], or for sensing with unwanted, yet important, "nuisance" parameters [20].

We are inspired by the classical fiber sensing technique of OTDR for our model sensor. The state-of-the-art in OTDR is to use embedded weak reflectors inside the fiber, dividing it into discrete sensing sections [21]. The time of arrival of each reflection gives distinguishing information on each section. Such measurements can be shot-noise limited [22], thus providing the potential for quantum techniques to enhance the measurement. We adapt this measurement to our model shown in Figure 1, with some modifications to effectively use squeezed light. In the sensing arm, $N - 1$ reflectors of transmission T separate N regions of the sensing arm, corresponding to an optical delay ϕ_i . On either side, 50:50 couplers form a Mach-Zehnder interferometer with bidirectional input. Circulators ensure that the detectors only see the output state of the interferometer. We use pulsed inputs in order to obtain distinguishing information on each phase.

Additionally, the interferometer takes squeezed light input from both sides, mixed with a laser, in order to minimize the impact of vacuum noise while not being photon-number limited. Each reflector is essentially a beamsplitter, with two inputs (left and right) and two outputs. Vacuum noise is introduced when squeezed light is on one beamsplitter input and vacuum is on the other, which reduces the squeezing strength. With squeezed light on both sides of each reflector for each reflection, squeezing strength is preserved; hence we need squeezed laser light from both left and right. To maintain synchronization of squeezed pulses, the delay between pulses is ideally the same as the propagation delay between reflectors. The resulting dynamics in the sensing arm of the interferometer are illustrated in Figure 1(b).

Modeling the sensor uses Gaussian states and operations commonly used in continuous-variable quantum information [23, 24]. A Gaussian state can be represented by a mean vector $\vec{R} = \{x, y\}$ and a covariance matrix σ . The vector \vec{R} represents the amplitude of the state in terms of the quadrature operators \hat{X} and \hat{Y} , which are accessible by homodyne detection. The matrix σ represents the quantum noise of that state. For example, a

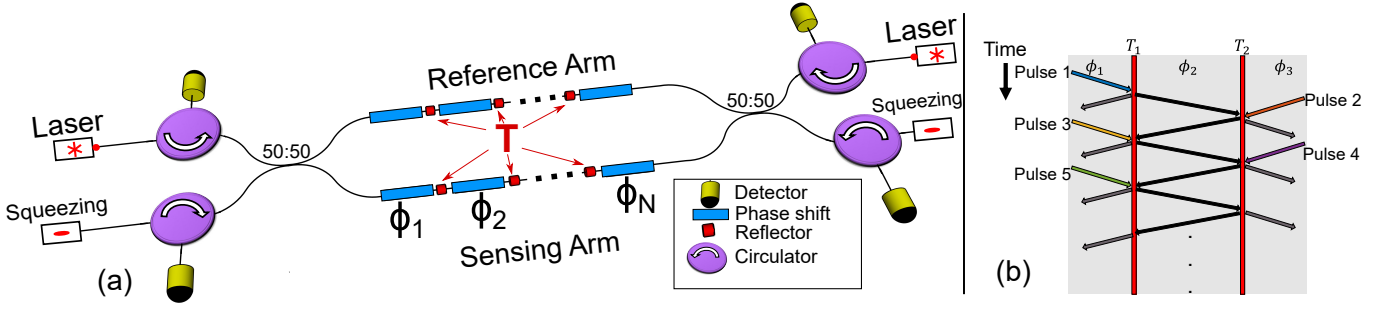


FIG. 1. (a) Layout of the sensor. N cascaded phases are separated by $N - 1$ evenly spaced reflectors of transmission T in the sensing arm. Balanced (50:50) couplers on either side form a Mach-Zehnder interferometer with bidirectional input. Circulators ensure that the detectors only see the output state of the interferometer. (b) Probe pulse dynamics within the sensing arm for a three-phase interferometer, demonstrating how multiple pulses interfere in the measurement. Pulses are introduced in a staggered fashion such that each reflection after the first has squeezed inputs on both sides, which eliminates vacuum noise in the system.

coherent state of strength α and phase θ will have:

$$\vec{R} = (|\sqrt{2}\alpha| \cos(\theta), |\sqrt{2}\alpha| \sin(\theta)), \quad (1)$$

$$\sigma_c = \mathbf{I},$$

where \mathbf{I} is the 2×2 identity matrix. In contrast, a squeezed coherent state may have the same amplitude but a different noise matrix:

$$\sigma_{\text{sq}} = \hat{S}(r, \chi) \hat{S}^\dagger(r, \chi), \quad (2)$$

$$\hat{S}(r, \chi) = \begin{pmatrix} \cosh(r) + \cos(\chi) \sinh(r) & \sin(\chi) \sinh(r) \\ \sin(\chi) \sinh(r) & \cosh(r) - \cos(\chi) \sinh(r) \end{pmatrix},$$

Here, $\hat{S}(r, \chi)$ is the single-mode squeezing operator with squeezing strength r and squeezing angle χ .

The sensor has many modes, both in space and time, and each are tracked separately in a multimode Gaussian state. An m -mode Gaussian state will have a longer mean vector $\vec{R} = \{x_1, y_1, x_2, y_2, \dots, x_m, y_m\}$ and a larger covariance matrix $\sigma_{2m, 2m}$. An initial state of this form propagates through a unitary matrix \mathbf{U} , representing the entire sensor. More details on constructing the unitary can be found in the supplementary material. The output state is:

$$\vec{R}_{\text{out}} = \mathbf{U} \cdot \vec{R}_{\text{in}} + \vec{d}, \quad (3)$$

$$\sigma_{\text{out}} = \mathbf{U} \cdot \sigma_{\text{in}} \cdot \mathbf{U}^\dagger + \mathbf{Y},$$

where \vec{d} is an added displacement and \mathbf{Y} represents any added noise [25].

Since the sensor is for multiparameter estimation, the Fisher information from a single parameter generalizes to a matrix for multiple parameters F_{ij} . Intuitively, diagonal elements F_{ii} indicate the amount of information obtained on a single parameter, while off-diagonal elements quantify the degree to which two parameters are

correlated in the output state. Assuming homodyne detection, the classical Fisher information matrix with respect to parameters ϕ_i and ϕ_j of a Gaussian state \vec{R}, σ takes the form [26]:

$$F_{ij} = 2 \frac{\partial \vec{R}^T}{\partial \phi_i} \cdot \sigma^{-1} \cdot \frac{\partial \vec{R}}{\partial \phi_j} + \frac{1}{4} \text{Tr}[\sigma^{-1} \cdot \frac{\partial \sigma}{\partial \phi_i} \cdot \sigma^{-1} \cdot \frac{\partial \sigma}{\partial \phi_j}] \quad (4)$$

The expression represents the classical Fisher information obtained from ideal homodyne detection on a pure Gaussian state [27]. Only with a pure state is the classical Fisher information equal to the quantum Fisher information [15]. Although a pure state is only possible with no optical losses, we separately document the effects of optical loss and added noise in the sensor in the supplementary material.

From the Fisher information matrix, we can get a lower bound on the sensitivity of measuring N phases with our novel sensor, which is the main result of this work. The sensitivity of each phase is constrained by the multiparameter Cramér-Rao bound [28]:

$$\Delta^2 \phi_i \geq (\mathbf{F}^{-1})_{ii}. \quad (5)$$

In words, the measurement variance on ϕ_i is bounded by diagonal element i in the inverse of the Fisher information matrix. Taking the inverse of F means that off-diagonal elements in F , representing correlated information between parameters, will generally increase the measurement variances of each parameter. If one has large Fisher information regarding two parameters, the measurement of those two parameters will still have large variance if those parameters appear highly correlated. Thus, it is not sufficient to maximize Fisher information; we must maximize *distinguishing* information.

Furthermore, Equations 4 and 5 apply equally to states with and without squeezing. If the measured parameters are partially separate, a squeezed state can still yield a quantum advantage. The squeezing angle and squeezing

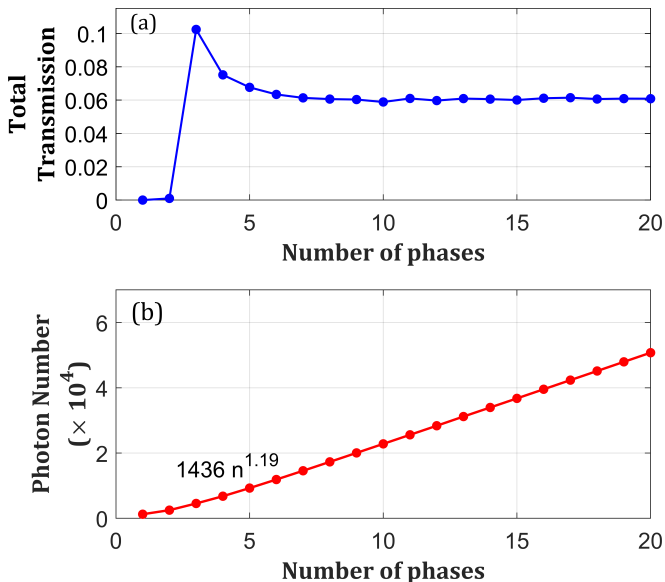


FIG. 2. Results of optimizing measurements in an interferometer with up to 20 phases with classical light. (a) The resulting total transmitted light in the interferometer is plotted as a function of N , showing that the total transmitted light in an optimal measurement quickly stabilizes near 6%. (b) The required photon number to maintain an average phase variance of 10 mrad in the sensor is plotted as a function of N . The photon number empirically scales as $N^{1.19}$, and such near-linear scaling shows that the sensor could handle many more phases.

strength in these states are additional degrees of freedom over classical light, and we use these degrees of freedom to further optimize phase sensitivity. The extra freedom in optimization gives some intuition on why quantum light can give enhanced sensitivity.

The trace of Eq. 5 is the total phase variance for a measurement in the sensor, and is the figure of merit by which we optimize the sensor’s sensitivity. With squeezed light, the sensitivity depends on each input pulse’s relative phase θ_i , squeezing angle χ_i , and the value of each phase in the reference arm $\phi_{r,i}$. We assume that the coherent state amplitude α_i is identical for each pulse and much larger than one. The reflector transmission T is also a variable, but the results are shown as a function of T in order to demonstrate the physics of the sensor.

For sensors with three or more phases, multiple embedded reflectors introduces the possibility of recursive reflections, essentially forming a weak cavity. In such cases, we truncate the total number of reflections each temporal mode can undergo to k and the number of input pulses to m . The truncation introduces some effective loss into the system, but taking $k \geq 7$ reduces loss to at most 5%. Truncation loss is also much lower if $T \approx 1$. Due to the many degrees of freedom in the sensor, a differential evolution algorithm was used to optimize its sensitivity [29]. We define the maximum expected im-

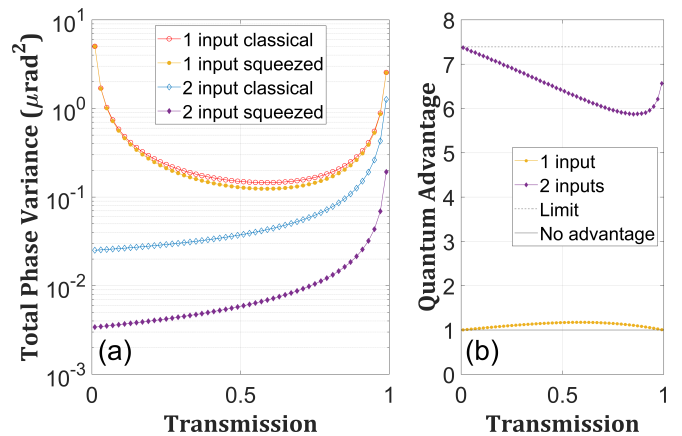


FIG. 3. Modeling results of measurements in a two-phase interferometer. Input parameters were set to $\alpha = 10^5$ and $r = 1$. (a) Total phase variance of the measurements is plotted as a function of reflector transmission T for one or bidirectional input and for classical or squeezed light. (b) Quantum advantage Q is plotted from the data in (a), showing a substantial advantage to using bidirectional input.

provement in measurement variance with quantum light will be Q , the quantum advantage:

$$Q = \frac{\sum_i \Delta^2 \phi_{i,\text{classical}}}{\sum_i \Delta^2 \phi_{i,\text{quantum}}} \leq e^{2r}. \quad (6)$$

To better show how the sensor architecture scales to more phases, simulations with up to 20 phases were performed with only classical light. Computational limitations prevented the use of squeezed light. All reflectors were set to have the same transmission. Figure 2(a) shows the fraction of light that would be transmitted through all reflectors, given that the reflectivity is optimized for minimum average phase variance. Remarkably, the total transmission quickly stabilizes to around 6%, suggesting that close to 94% of the light should be reflected at least once for an optimal design. Moreover, to show the scaling potential for sensing many phases, we calculated the photon number required to maintain an average phase uncertainty of 10 mrad as the number of phases increased. Results are shown in Figure 2(b), showing that the required photon number scales as low as $n^{1.19}$. Therefore, with almost linear scaling of input power, one could sense many more phases with the sensor.

The general N -phase system will have some effective loss of squeezing. The first pulse must first pass through at least half of the interferometer before interacting with pulses input from the other side, and the reflectors on the way introduce vacuum noise into the pulse. Adding more squeezed pulses should asymptotically overcome the vacuum noise. We speculate that about $m = 3N$ pulses will be needed to approach the e^{2r} improvement limit. This asymptotic behavior will be demonstrated in the 3

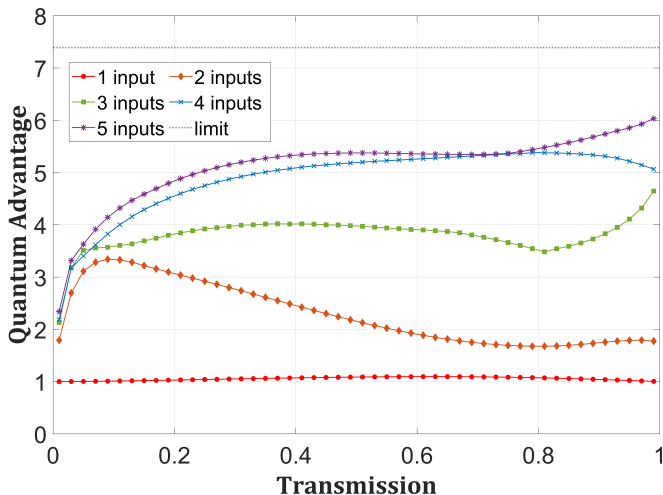


FIG. 4. Modeling results of the three-phase interferometer, showing the improvement in measurement sensitivity with an optimal multiparameter measurement with a squeezed coherent state over that of the same measurement with the same amount of classical light. Input parameters were set to $\alpha = 3 \times 10^4$ and $r = 1$ for each pulse. The quantum advantage Q is plotted as a function of reflector transmission T for up to five input pulses. The quantum advantage, Q , is shown to increase with more input pulses, asymptotically approaching the limit set by the amount of vacuum noise in the system.

phase example below. Therefore, our sensor is potentially scalable to many phases so long as one can generate the appropriate sequence of pulses.

An illustrative example of the sensor operation is the simplest case: the two-phase interferometer, with a single reflector. We compare the total measurement variance as a function of reflector transmission for four different iterations: one input (from the left in Figure 1) or two inputs (from both directions), and with either a coherent state or a squeezed coherent state. The coherent state indicates the performance of the sensor with classical light, while the squeezed coherent state indicates performance with quantum light.

Results are shown in Figure 3. First, compare the two cases with one input. With both classical and quantum input, the total measurement variance diverges at $T = 0$ and at $T = 1$. Near $T = 0$, the divergence is due to a very weak measurement on ϕ_2 , since very little light transmits through the reflector to pass through ϕ_2 . Near $T = 1$, distinguishing information on each phase diminishes to zero, which is also true for an N -phase sensor. Moreover, in Figure 3(b), the quantum advantage from a single input is at most 17% near $T = 0.63$. The low advantage is due to the reflector introducing vacuum noise into the state, effectively reducing the squeezing strength for the measurement.

The two-input, or bidirectional input case, shows substantially more promise. While the measurement vari-

ances still diverge near $T = 1$ for the same reason as before, they do not near $T = 0$. At that point, the system is essentially two separate interferometers, each independently measuring ϕ_1 or ϕ_2 . The quantum advantage correspondingly starts at its limit near $T = 0$. Interestingly, the quantum advantage remains high for all T because squeezed light is interfering with additional squeezed light at the reflector, instead of vacuum noise. Thus, there is no effective loss of squeezing. The quantum advantage for intermediate values of T is slightly lower because the optimal points for measuring ϕ_1 and ϕ_2 are different. Thus, the chosen measurement makes some compromise between the two. Despite the two phases being nearly inseparable in the output state, one can still measure both simultaneously with a substantial quantum advantage. The general key here is to avoid any interaction with vacuum noise by introducing additional squeezed light at every reflector such that light from two directions interfere.

A three-phase interferometer is more representative of the general N -phase system due to the use of multiple synchronized pulses and multiple reflections. The quantum advantage will be a function of the number of input pulses m as well as the reflector transmission T . Results for the three-phase interferometer as a function of the number of input pulses m are shown in Figure 4. We tracked $k = 7$ reflections for each temporal mode, and set $\alpha = 3 \times 10^5$. Similar to the analysis of the two-phase interferometer, we show the quantum advantage from using a varying number of inputs. A single input gives a Q of at most 9.5% at $T = 0.62$. However, with a second input, the light has one fewer interactions with vacuum noise, and so the sensor shows a stronger quantum advantage. Similarly, a third input removes one more interaction with vacuum noise, and so the improvement is stronger still. With more input pulses, this trend will continue until the sensor hits a saturation point near e^{2r} .

We have developed the framework for a new branch of quantum metrology we call cascaded phase sensing. Our novel structure features evenly spaced reflectors on the sensing path for defining phase sensing regions, and bidirectional input for effective use of squeezed light. Despite the cascaded phases sharing an optical path, we show that squeezed light can give close to a full quantum advantage in phase sensing. While we show this enhancement for two and three phases, the same physics applies to sensors with many more phases. Our sensing protocol offers a new perspective for distributed fiber sensing as well as multiparameter quantum metrology. This methodology has applications in remote sensing, calibration of networks in quantum communications, and in geophysics.

We acknowledge useful technical discussions with Joshua Combes, Krister Shalm, Michael MESSERLY, Stephen Libby, and Robert Mellors. We gratefully acknowledge funding from ARPA-E, DE-AR0001152, NSF

CCF 1838435, and the University of Colorado Boulder Cubit initiative.

-
- [1] C. M. Caves, Quantum-mechanical noise in an interferometer, *Phys. Rev. D* **23**, 1693 (1981).
- [2] V. Giovannetti, S. Lloyd, and L. Maccone, Quantum-Enhanced Measurements: Beating the Standard Quantum Limit, *Science* **306**, 1330 (2004).
- [3] J. P. Dowling and K. P. Seshadreesan, Quantum Optical Technologies for Metrology, Sensing, and Imaging, *Journal of Lightwave Technology* **33**, 2359 (2015), [arXiv:1412.7578](#).
- [4] T. L. S. Collaboration, Enhanced sensitivity of the LIGO gravitational wave detector by using squeezed states of light, *Nature Photonics* **7**, 613 (2013), [arXiv:1310.0383](#).
- [5] M. A. Taylor, J. Janousek, V. Daria, J. Knittel, B. Hage, H.-A. Bachor, and W. P. Bowen, Biological measurement beyond the quantum limit, *Nature Photonics* **7**, 229 (2013), [arXiv:1206.6928](#).
- [6] B.-B. Li, J. Bílek, U. B. Hoff, L. S. Madsen, S. Forstner, V. Prakash, C. Schäfermeier, T. Gehring, W. P. Bowen, and U. L. Andersen, Quantum enhanced optomechanical magnetometry, *Optica* **5**, 850 (2018).
- [7] X.-Q. Xiao, E. S. Matekole, J. Zhao, G. Zeng, J. P. Dowling, and H. Lee, Enhanced phase estimation with coherently boosted two-mode squeezed beams and its application to optical gyroscopes, *Physical Review A* **102**, 022614 (2020).
- [8] C. You, S. Adhikari, Y. Chi, M. L. LaBorde, C. T. Matyas, C. Zhang, Z. Su, T. Byrnes, C. Lu, J. P. Dowling, and J. P. Olson, Multiparameter estimation with single photons—linearly-optically generated quantum entanglement beats the shotnoise limit, *Journal of Optics* **19**, 124002 (2017).
- [9] E. Polino, M. Riva, M. Valeri, R. Silvestri, G. Corrielli, A. Crespi, N. Spagnolo, R. Osellame, and F. Sciarrino, Experimental multiphase estimation on a chip, *Optica* **6**, 288 (2019).
- [10] Z. Hou, Z. Zhang, G.-Y. Xiang, C.-F. Li, G.-C. Guo, H. Chen, L. Liu, and H. Yuan, Minimal tradeoff and ultimate precision limit of multiparameter quantum magnetometry under the parallel scheme, *Phys. Rev. Lett.* **125**, 020501 (2020).
- [11] M. D. Vidrighin, G. Donati, M. G. Genoni, X.-M. Jin, W. S. Kolthammer, M. Kim, A. Datta, M. Barbieri, and I. A. Walmsley, Joint estimation of phase and phase diffusion for quantum metrology, *Nature Communications* **5**, 3532 (2014), [arXiv:1410.5353](#).
- [12] D. Šafránek, Estimation of Gaussian quantum states, *Journal of Physics A: Mathematical and Theoretical* **52**, 035304 (2019), [arXiv:1801.00299](#).
- [13] W. Górecki and R. Demkowicz-Dobrzański, Multiple-phase quantum interferometry: Real and apparent gains of measuring all the phases simultaneously, *Phys. Rev. Lett.* **128**, 040504 (2022).
- [14] Q. Zhuang, Z. Zhang, and J. H. Shapiro, Distributed quantum sensing using continuous-variable multipartite entanglement, *Phys. Rev. A* **97**, 032329 (2018).
- [15] C. Oh, C. Lee, S. H. Lie, and H. Jeong, Optimal distributed quantum sensing using Gaussian states, *Physical Review Research* **2**, 023030 (2020), [arXiv:1910.00823](#).
- [16] X. Guo, C. R. Breum, J. Borregaard, S. Izumi, M. V. Larsen, T. Gehring, M. Christandl, J. S. Neergaard-Nielsen, and U. L. Andersen, Distributed quantum sensing in a continuous-variable entangled network, *Nature Physics* **16**, 281 (2020), [arXiv:1905.09408](#).
- [17] P. Kómár, E. M. Kessler, M. Bishof, L. Jiang, A. S. Sørensen, J. Ye, and M. D. Lukin, A quantum network of clocks, *Nature Physics* **10**, 582 (2014), [arXiv:1310.6045](#).
- [18] P. Lu, N. Lalam, M. Badar, B. Liu, B. T. Chorpene, M. P. Buric, and P. R. Ohodnicki, Distributed optical fiber sensing: Review and perspective, *Applied Physics Reviews* **6**, 041302 (2019).
- [19] T. J. Proctor, P. A. Knott, and J. A. Dunningham, Multiparameter estimation in networked quantum sensors, *Phys. Rev. Lett.* **120**, 080501 (2018).
- [20] J. Suzuki, Y. Yang, and M. Hayashi, Quantum state estimation with nuisance parameters, *Journal of Physics A: Mathematical and Theoretical* **53**, 453001 (2020), [arXiv:1911.02790](#).
- [21] B. Redding, M. J. Murray, A. Donko, M. Beresna, A. Masoudi, and G. Brambilla, Low-noise distributed acoustic sensing using enhanced backscattering fiber with ultra-low-loss point reflectors, *Optics Express* **28**, 14638 (2020).
- [22] M. Wu, X. Fan, Q. Liu, and Z. He, Quasi-distributed fiber-optic acoustic sensing system based on pulse compression technique and phase-noise compensation, *Optics Letters* **44**, 5969 (2019).
- [23] G. Adesso, S. Ragy, and A. R. Lee, Continuous Variable Quantum Information: Gaussian States and Beyond, *Open Systems and Information Dynamics* **21**, 1440001 (2014).
- [24] A. Serafini, *Quantum Continuous Variables* (CRC Press, Boca Raton, FL : CRC Press, Taylor and Francis Group, [2017] —, 2017).
- [25] K. Sharma, B. C. Sanders, and M. M. Wilde, Optimal tests for continuous-variable quantum teleportation and photodetectors, *Physical Review Research* **4**, 023066 (2022).
- [26] D. Šafránek, Estimation of Gaussian quantum states, *Journal of Physics A: Mathematical and Theoretical* **52**, 035304 (2019), [arXiv:1801.00299](#).
- [27] C. Oh, C. Lee, C. Rockstuhl, H. Jeong, J. Kim, H. Nha, and S.-Y. Lee, Optimal Gaussian measurements for phase estimation in single-mode Gaussian metrology, *npj Quantum Information* **5**, 10 (2019), [arXiv:1805.08495](#).
- [28] S. Ragy, M. Jarzyna, and R. Demkowicz-Dobrzański, Compatibility in multiparameter quantum metrology, *Phys. Rev. A* **94**, 052108 (2016).
- [29] R. Storn and K. Price, A Simple and Efficient Heuristic for global Optimization over Continuous Spaces, *Journal of Global Optimization* **11**, 341 (1997).